Lab on a Chip

PAPER

View Article Online
View Journal | View Issue

Cite this: *Lab Chip*, 2021, **21**, 2040

Measuring barrier function in organ-on-chips with cleanroom-free integration of multiplexable electrodes†

Elsbeth G. B. M. Bossink, ‡* Mariia Zakharova, ‡* Douwe S. de Bruijn, Mathieu Odijk and Loes I. Segerink

Transepithelial/transendothelial electrical resistance (TEER) measurements can be applied in organ-on-chips (OoCs) to estimate the barrier properties of a tissue or cell layer in a continuous, non-invasive, and label-free manner. Assessing the barrier integrity in *in vitro* models is valuable for studying and developing barrier targeting drugs. Several systems for measuring the TEER have been shown, but each of them having their own drawbacks. This article presents a cleanroom-free fabrication method for the integration of platinum electrodes in a polydimethylsiloxane OoC, allowing the real-time assessment of the barrier function by employing impedance spectroscopy. The proposed method and electrode arrangement allow visual inspection of the cells cultured in the device at the site of the electrodes, and multiplexing of both the electrodes in one OoC and the number of OoCs in one device. The effectiveness of our system is demonstrated by lining the OoC with intestinal epithelial cells, creating a gut-on-chip, where we monitored the formation, as well as the disruption and recovery of the cell barrier during a 21 day culture period. The application is further expanded by creating a blood–brain-barrier, to show that the proposed fabrication method can be applied to monitor the barrier formation in the OoC for different types of biological barriers.

Received 18th December 2020,
Accepted 4th April 2021

DOI: 10.1039/d0lc01289k

rsc.li/loc

Introduction

Organ-on-chips (OoCs) are defined as microfluidic cell culture devices that mimic organ-specific functions.[1] These devices are a potential alternative to conventional animal and *in vitro* models for drug screening as OoCs are able to emulate complex human physiology in a miniaturized and highly controlled environment.[2–4] OoCs are often made from biologically inert polymers such as polydimethylsiloxane (PDMS) and contain two parallel microfluidic culture channels, separated by a porous membrane, lined with organ-specific cell types.[4,5] By integrating a porous membrane, barrier tissues can be studied which are essential for maintaining homeostasis of the organs and regulating the transport of certain compounds.[6] Assessment of barrier integrity in such *in vitro* model provides valuable information for further clinical studies and barrier targeting drug development.[7] One of the ways to access the barrier properties is to study the transepithelial/transendothelial electrical resistance (TEER) of the barrier or monolayer. TEER provides a continuous, non-invasive, and label-free way of monitoring the tightness of cell–cell junctions by measuring the electrical resistance across a cellular barrier.[8]

The EVOM2 volt/ohmmeter is a commercially available device that is often used to measure barrier function in conventional *in vitro* models, such as the Transwell system.[9] The device has 'chopstick' type electrodes, which are introduced on both sides of the Transwell insert. The resistance of the path between the electrodes, also through the cell layer, is measured by applying a direct or alternating current (DC or AC).[10] This 'chopstick method' is also applied for typical OoC devices, by placing the electrodes in the in- and outlets of the opposite microfluidic channels.[11,12] However, this method raises concerns about the stability of the electrode position and the membrane area that is actually probed,[13,14] making it very difficult to obtain reliable and representative measurements.

Alternatively, integrated TEER electrodes in OoCs have been already reported.[15–21] Using advanced microfabrication technologies, miniaturized sensors can be directly embedded in, or in close proximity to the cell culture channels. This was accomplished by patterning electrodes on the top and bottom substrates of the channels.[16,17,22] Although these methods provide stable and reliable TEER measurements,

BIOS Lab on a Chip Group, MESA+ Institute for Nanotechnology, Technical Medical Center and Max Planck Institute for Complex Fluid Dynamics, University of Twente, The Netherlands. E-mail: e.g.b.m.bossink@utwente.nl, m.zakharova@utwente.nl

† Electronic supplementary information (ESI) available. See DOI: 10.1039/d0lc01289k

‡ These authors contributed equally.

the electrodes block the possibility for visual inspection of the cells at the site of the electrode. This issue has been solved by using very thin electrodes of gold[19] or indium tin oxide.[15] However, these fabrication methods are based on the sputtering of electrodes, an expensive process often requiring cleanroom access.

Therefore, methods for integrating TEER electrodes in OoCs are developed that do not require cleanroom facilities. A simple, but elegant and cleanroom-free way to integrate platinum electrode wires horizontally in a microfluidic device has already been reported.[20] Using four platinum wires, the TEER is measured in a blood–brain barrier (BBB) on-chip. The special configuration of the four electrodes allows to obtain 6 measurements to remove large variations of non-biological origin. However, such configuration is only compatible with the proposed device design (containing two crossed channels) making it difficult to apply to a typical PDMS OoC device (containing two parallel channels). Moreover, the area of interest between two crossing channels is very small (0.5 mm × 0.5 mm), limiting the possible readouts. Furthermore, the method is not applicable to a multi-chamber or multiplexed OoC. Scaling up the number of microfluidic chambers in one device will allow parallel experiments and analysis of multiple conditions thereby increasing the throughput per device. We would ideally have a method to study the TEER in a typical PDMS OoC with a cleanroom-free fabrication method, which allows parallelization and the visual inspection of the cells in the device. This has, to our knowledge, not been shown yet.

Here, a cleanroom-free fabrication method for the integration of platinum electrode wires is presented which allows real-time measurement of the barrier resistance in a PDMS OoC by means of impedance spectroscopy. With the proposed configuration, it is possible to multiplex both the electrodes and the OoCs in one device and simultaneously be able to visually inspect the culture channel at the site of the electrodes. To illustrate the applicability of the new method, a PDMS device with three parallel OoC units was fabricated and lined with Caco-2 cells to mimic the intestinal epithelium in a gut-on-chip. We monitored and observed the formation, as well as the disruption of the cell–cell barrier in the gut-on-chip during cell culture both visually and by impedance spectroscopy. To expand the application of the fabrication method, we also measured the barrier formation in a chip lined with brain endothelial cells, hCMEC/D3 cells, to mimic the BBB. We demonstrate that the proposed fabrication method can be applied to monitor the barrier formation in a PDMS two-layer OoC device with different types of biological barriers.

Material and methods

Chip fabrication

A schematic illustration of the chip is shown in Fig. 1. Two polymethylmethacrylate (PMMA) molds for top and bottom channels were designed in a 3D-CAD software (SolidWorks®, 2018) and micromilled (Datron Neo, Germany). PDMS base and curing agent were mixed (10 : 1% w/w, Sylgard 184 Silicone elastomer kit, Dow Corning) and degassed. The PDMS was cast on the two PMMA molds and cured for 4 hours at 60 °C. In- and outlets were punched in the PDMS top layer with a 1 mm biopsy puncher (Ted Pella Inc., US). The inlets for the platinum electrodes (E1–E4) were punched with a 0.5 mm puncher (Harris Uni-Core™, *via* Sigma-

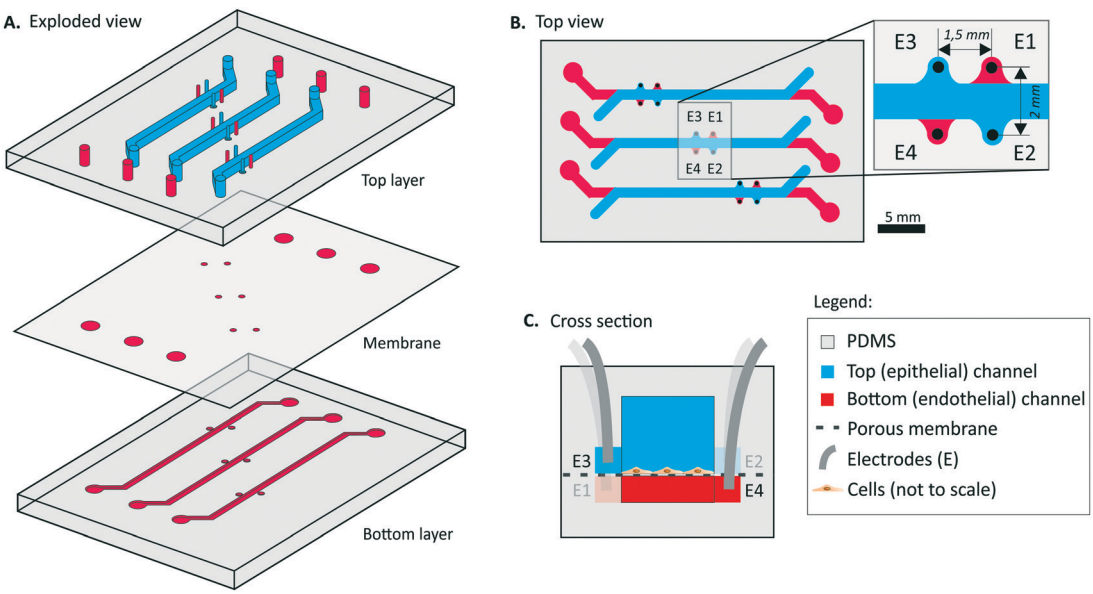

Fig. 1 Schematic illustration of the multiplexed PDMS microfluidic chip with 3 individual OoCs with electrode wells A) exploded view. B) Top view of the chip, with an indication of the 4 electrodes (E1–E4) per OoC. The total culture area with overlapping top (epithelial) and bottom (endothelial) channel is 19 mm^2. Both top and bottom channels are 1 mm wide. C) Schematic cross-section of the OoC at the site of the electrodes E3 and E4 with corresponding electrode indications (E1–E4). The top and bottom channels are 1 mm and 0.2 mm high respectively.

Aldrich). After punching, any potential dust at the surface was removed using Scotch tape.[23] A PDMS membrane with a thickness of 2 μm and 5 μm pore size, was fabricated based on our previously developed protocol.[24] Briefly, an array of columns was formed with positive photoresist (PR) (AZ 9260) using a standard soft-lithography technique. Next, a solution of PDMS: hexane (2 : 5% w/w) was spin-coated on top of the wafer with PR columns and cured for 4 hours. Finally, the PR was removed with acetone, releasing the membrane which was bonded by oxygen plasma treatment (40 seconds, 50 Watt, Femto Science, Cute) to the PDMS top layer. The PDMS membrane was removed from the inlets of the bottom channel, and the electrode holes for the bottom channel (E1 and E4) to provide proper access. Next, the bottom layer was bonded to the membrane and top layer using oxygen plasma. The chips were carefully visually checked for membrane integrity after the assembly and during the cell culture period.

Four platinum wires (0.25 mm diameter, Alfa Aesar, Thermo Fisher Scientific) were cleaned and inserted in the pre-punched holes and secured using UV curable glue (NOA 86H, Norland Products), based on earlier work.[23] The platinum electrodes could also be attached at another site onto the PDMS chip, to prevent the electrodes from being pulled out of the punched holes during cell culture. To completely cure the NOA, the chips were baked for 4 hours at 60 °C.

Cell culture

The fabricated device was used to model two biological barriers; the intestinal barrier and the BBB to measure the transepithelial and transendothelial electrical resistance, respectively. Human caucasian colon adenocarcinoma (Caco-2) cells were used to create a gut-on-chip. This well-differentiated cell line is commonly used for *in vitro* modeling intestinal barriers due to its ability to form tight junctions between cells, resulting in a tight epithelial barrier.[25,26] Furthermore, the cell line can spontaneously differentiate to different intestinal cell types and form villi when cultured on-chip under flow and peristalsis-like deformation.[27] For modeling the blood–brain barrier, the commercially available human cerebral microvascular endothelial (hCMEC/D3) immortalized cell line was chosen. The hCMEC/D3 cells have previously shown to express various important functional parameters of relevance to barrier tightness such as zonula occludens-1 (ZO-1), VE-cadherin and claudin-5 (ref. 28 and 29) and showed the applicability for drug transport studies.[30,31]

Gut-on-chip: Caco-2 cells. The Caco-2 cells (ATCC, HTB-37, Caco-2 cell line) were cultured in Dulbecco's modified Eagle's medium (DMEM) high glucose Glutamax medium (Gibco), supplemented with 20% fetal bovine serum (FBS, Gibco), 100 U L^{-1} penicillin, and 100 μg mL^{-1} streptomycin. The cells were cultured in T25 or T75 culture flasks and incubated at 37 °C in humidified air (5% CO_2).

Before cell seeding, the PDMS chips were treated with oxygen plasma (40 seconds, 50 Watt, Femto Science, Cute), flushed with 70% ethanol (Boom, The Netherlands), and subsequently flushed with phosphate-buffered saline (PBS, Sigma-Aldrich). The channels were coated with 100 μg mL^{-1} collagen-I (Gibco) in PBS for 30 minutes at 37 °C. The collagen solution was replaced by cell culture medium and the chips were incubated for an additional 2 hours at 37 °C and 5% CO_2.

Caco-2 cells were obtained from a T75 flask grown until almost confluent, using 1× trypsin (Gibco) and resuspended in the cell culture medium. Caco-2 cells (passage number 30 or 31) were seeded in the top (epithelial) culture channels with a cell density of 5×10^4 cells per cm^2. After seeding, the chips were incubated for 1 hour at 37 °C to adhere. Subsequently, the cell medium was replaced by placing empty 200 μL pipette tips in the outlet and 200 μL pipette tips filled with the medium in the inlets.

The cell culture on-chip was maintained for 8 or 21 days (at 37 °C, 5% CO_2) and cells were monitored by using phase-contrast microscopy (EVOS, M5000 Imaging system, Life Technologies air objectives). At day 21, images were also taken with a brightfield microscope (Olympus IX51) equipped with a color CCD camera (FLIR Grasshopper3, U232S6C). The exact same procedure was followed for chips, without the cell seeding step described in the previous paragraph. These blank chips were incubated at 37 °C, 5% CO_2 for 22 days as a control study.

BBB-on-chip: hCMEC/D3 cells. The hCMEC/D3 cells were cultured in endothelial cell growth medium (EGM) in T75 culture flasks and incubated at 37 °C in humidified air (5% CO_2). The sterilization, coating (collagen-I, Corning) and seeding protocol for the chip were similar as previously described for the Caco-2 cells. The hCMEC/D3 cells (passage number 31–35) were seeded at a seeding density 2×10^5 cells per cm^2 in the bottom (endothelial) channels of the collagen-coated chips. The chip was then immediately inverted so the cells could attach on another side of the membrane and left in the incubator (37 °C, 5% CO_2) for 1 hour. Subsequently, the chips were inverted back, and the fresh medium was introduced into each channel to flush non-attached cells. The cell culture was maintained for 4 days and the medium was refreshed every day by replacing the pipette tips with fresh medium. For the control measurements, blank chips were prepared by following the protocol without the hCMEC/D3 cell seeding step.

Immunofluorescence staining

Gut-on-chip: Caco-2 cells. Immunofluorescence staining was performed on the 7th, 8th or 21st day of culture. The Caco-2 cells were fixed with 4% (v/v) paraformaldehyde (Thermofisher) for 20 minutes at room temperature (RT) followed by permeabilization with 0.1% Triton X-100 (Sigma-Aldrich) and blocking with 5% Bovine serum albumin (BSA, Sigma-Aldrich) solution in PBS for 1 hour. Subsequently, to

visualize tight junctions, the Caco-2 cells were incubated with primary rabbit anti-ZO-1 (1 : 100, polyclonal, Invitrogen) diluted in 1% BSA solution overnight at 4 °C. Next, the cells were rinsed three times with PBS and the secondary antibody (Alexa Fluor 647 goat anti-rabbit, dilution 1 : 500, Invitrogen) was introduced. The samples were protected from light and left at RT for 1 hour. The cell nuclei were stained with DAPI (NucBlue™ Fixed Cell ReadyProbes™ Reagent, Thermo Fisher Scientific) at RT for 20 minutes. Images were acquired using a confocal microscope (Nikon Instruments A1 Confocal Laser Microscope) with 10× air objective.

BBB-on-chip: hCMEC/D3 cells. The hCMEC/D3 cells were stained after 4 days of culture on-chip. The staining of the adherens junctions marker-vascular endothelial cadherin (VE-cadherin) and tight junction protein marker ZO-1 followed the same procedure as for Caco-2 cells. After fixing and permeabilizing cells, the primary rabbit anti-ZO-1 (1 : 100, polyclonal, Invitrogen) and primary mouse VE-cadherin (1 : 100, Santa Cruz Biotechnology) were diluted in 0.5% BSA and incubated at 4 °C overnight. Subsequently, the cells were washed 3 times with PBS and incubated with the secondary antibodies (Alexa Fluor 647 goat anti-rabbit and Alexa Fluor 488 goat anti-mouse dilution 1 : 500, Invitrogen) for 1 hour at RT. The cell nuclei were stained with DAPI (NucBlue™ Fixed Cell ReadyProbes™ Reagent, Thermo Fisher Scientific) at RT for 20 minutes. The fluorescence images were taken using a confocal microscope (Nikon Instruments A1 Confocal Laser Microscope) with 10× air objective.

Intestinal barrier disruption

On day 7 or day 19, the Caco-2 cells were treated with a solution of 5 mM EGTA (ethylene glycol-bis(β-aminoethyl ether)-*N*,*N*,*N*′,*N*′-tetraacetic acid, Sigma-Aldrich), in PBS for 45 minutes. EGTA is a calcium (Ca^{2+}) chelator, which will affect the adherens and tight junctions of the cells, resulting in loss of barrier function.[17] Subsequently, the cells were incubated in cell culture medium to study the recovery of the barrier function. After 30 minutes, 1 hour and overnight incubation in DMEM, impedance measurements were performed.

Impedance spectroscopy

Prior to measuring, the cell culture medium in every compartment of the chip was replaced with DMEM or EGM at RT by gravity-driven flow, inserting empty 200 µl pipette tips at the outlets and 200 µl pipette tips filled with RT DMEM or EGM at the inlets. Impedance spectra were recorded daily using the Zurich Instruments HF2IS Impedance Spectroscope or a HF2LI lock-in amplifier (both Zurich Instruments, Switzerland). The impedance was recorded using an alternating (AC) signal with an amplitude of 0.1 V for six combinations of the four electrodes indicated in Fig. 1 (electrode combinations: E1–E2, E1–E3, E1–E4, E2–E3, E2–E4, and E3–E4) at a frequency range of 100 Hz–1 MHz, as previously described.[20] Before performing the frequency sweep, the impedance magnitude at 1 MHz was checked to ensure correct connection of the electrodes. After recording the impedance spectra, warm cell culture medium (37 °C) was inserted and the chips were placed in an incubator (37 °C, 5% CO_2). At day 0, the impedance spectra were recorded twice, before and after cell seeding. For the intestinal barrier disruption and recovery at day 7 or day 19, the spectra were measured five times for the gut-on-chips (before EGTA treatment in DMEM and in PBS, after EGTA treatment in PBS, after 30 minutes of incubation with DMEM and after 60 minutes of incubation with DMEM).

The measured data was processed in MATLAB (version R2017b) and TEER was obtained by determining a suitable readout frequency from the impedance and phase plots. The information of the cell barrier was found from the four measurements between top-bottom electrode pairs, which measure through the PDMS membrane and cell layer (electrode pairs E1–E2, E1–E3, E2–E4, and E3–E4). The magnitudes of these four electrode pairs were averaged for each session and hereinafter referred to as $|Z_{\text{average}}|$. To obtain solely the information attributed to the growing cell layer, the magnitudes of each electrode pair of the measurements prior to cell seeding ($|Z_{\text{average day0}}|$) were subtracted from all the subsequent measurements during cell culture ($|Z_{\text{average day\#}}|$), resulting in the relative magnitude ($|Z_{\text{relative}}|$). At day 7 or day 19 the measurements before EGTA treatment were performed in DMEM and PBS to ensure a fair comparison in relative impedance change during the disruption and recovery event. The conductivity of PBS and DMEM are similar, therefore the same readout frequency was used.

Results and discussion

Fabricated chip

We designed a microfluidic OoC device that consists of two PDMS parts separated by a 2 µm-thick, porous (pore size 5 µm, pitch 30 µm) PDMS membrane and the device contains three parallel cell culture chambers (Fig. 2). The PDMS thin

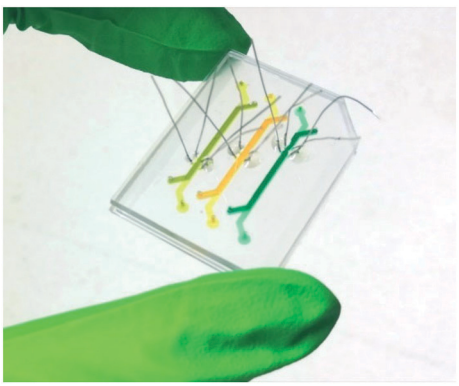

Fig. 2 The final fabricated microfluidic device with three independent OoCs and three sets of four electrodes integrated in each OoC. The OoCs have a 19 mm^2 cross-sectional area between the top and bottom channels. The channels are filled with different colors of food dye. The PDMS device outer dimensions are 40 × 30 mm.

membrane stayed intact over the cell culture period and allowed a clear visual inspection of the cells, however, its fabrication requires a cleanroom. When a completely cleanroom-free fabrication method is preferred, the thin PDMS membrane can be replaced by a commercially available polyester or polycarbonate membrane[23] or a cleanroom-free PDMS membrane.[32] The fabrication of such completely cleanroom-free TEER chip is described and shown in ESI† S5. The cell culture chambers of the OoC were each 1 mm wide with a 1 mm high and 24 mm long top (epithelial) channel and a 0.2 mm high and 30 mm long bottom (endothelial) channel. The complete device can be assembled by only using a plasma activation of the PDMS parts and does not require additional glues for bonding the membrane. The 4 electrodes were inserted on the sides of the channel in the assembled chip and fixed with a NOA glue, securing the position of the electrodes, therefore eliminating measurement errors due to variation in electrode placement between measurements,[13,14] which can occur when inserting wires manually to the in/outlets. After applying, the glue filled the punched holes with the electrodes and it was immediately cured with the UV-lamp to prevent complete coverage of the electrodes and leakage to the culture chamber. Fig. S1† shows a cross-section of the placement of the electrodes in the PDMS chip.

The electrode arrangement allows inspection of the cells inside the culture channels at the site of the electrodes and the electrodes can be easily multiplexed, as demonstrated by the presence of 3 independent OoCs in Fig. 2 highlighted by yellow, orange and green food dye.

The proposed method of electrode integration can also be used for wires consisting of other materials, such as ruthenium oxide coated platinum wires or silver/silverchloride wires, which can allow other types of electrical measurements (for measuring *e.g.* pH, nitric oxide or oxygen) and simultaneously still facilitate impedance spectroscopy.[33–37]

Gut-on-chip

Typical impedance spectra for a blank chip and a chip with Caco-2 cells are shown in Fig. 3A and B respectively. At approximately 2 kHz the maximum difference in the impedance spectra of an empty chip compared to a chip with a confluent cell layer was seen and therefore this was chosen as readout frequency (Fig. S2A and B†). This readout frequency also corresponds with the crossing point of the phase plot for a blank chip and chip with cells (Fig. S2A†); a method of determining the TEER that was reported previously.[38] The measurement of day 0 (of an empty chip) before adding cells, was subtracted from all subsequent measurements (resulting in the $|Z_{\text{relative}}|$) to see the change in impedance exclusively attributed to the cell layer.

The relative impedance $|Z_{\text{relative}}|$ at 2 kHz is monitored in chips with and without Caco-2 cells over 21 days of culture (Fig. 3C). Measurements of all six electrode pairs over time in a single chip with and without cells are shown in Fig. S3.† In the chips without cells, blank chips, Fig. 3C shows that no barrier formation was measured. A relative stable impedance is observed as expected, as the resistance of the system should not change over time. One blank chip is excluded from the graph after day 17, as leakage at the chip's in- and outlet was observed. In the chips with Caco-2 cells the measured $|Z_{\text{relative}}|$ kept increasing during all 21 days of culture following a similar trend for both chips and they reached a maximum value of 13 kΩ for chip 1 and 9.3 kΩ for chip 2.

Conventionally, TEER values are presented in Ω cm^2. In our work, the measured barrier function is expressed in Ω, since not the whole membrane culture area is probed, due to the placement of the electrodes. The TEER in Ω cm^2 can be estimated by multiplying the results in Ω by 0.04 cm^2, which is approximately the culture area between the four electrode wells (Fig. 1B) we assume to be dominantly probed by the electrodes. However, it is important to keep in mind that the actual probed area might be larger than the 0.04 cm^2 when the barrier is fully formed and also specific parts of the membrane will have a larger effect on the measured value than others.[17] Also, the probing area can change over time, as it is affected by the cell layer resistance.[19] To facilitate the comparison with TEER values between studies, we added the estimated TEER values in Ω cm^2 at the right axis of Fig. 3C.

Nevertheless, it is not trivial to compare the obtained TEER values (in Ω cm^2) to absolute values reported in the literature, and there is also no consensus about the 'real' absolute TEER values for Caco-2 cells.[11,19,21,25,39–41] This can be explained by the various factors influencing TEER measurements such as: the culture systems used (Transwell or microfluidic chip), the cell culture/probing area, the temperature during measurement, the applied potential (AC/DC), the electrolyte, the measuring system and position of the electrodes (chopsticks, electrodes integrated in the microfluidic channels, platinum or silver/silver chloride electrodes), and the analysis method (calculation of the TEER, the readout frequency, normalization, relative magnitudes). Furthermore, it is important to understand that when selecting a single readout frequency in such complex biological models, a TEER value can only give a reasonable approximation and not a precise indication of solely the barrier formation. We want to stress the complexity of the equivalent electrical model and the effect of all its components on the impedance. There is no signal frequency that will tell solely about the resistance of the cell layer, because of the various components and processes in the OoC (*e.g.* 3D villi formation can add to the measured impedance, which is then incorrectly related to the R_{teer} value).[38,42] Due to these factors different studies show varying absolute measured TEER values for Caco-2 cells cultured in both Transwell systems and chips and caution should be taken when comparing the TEER values.

Béduneau *et al.* presented a gradual increase in cell barrier (or TEER) for the first 20 days in a Transwell study with Caco-2 cells, up to a TEER of approximately 450 Ω cm^2,[39] which is similar as we see in our culture. However, they did not report

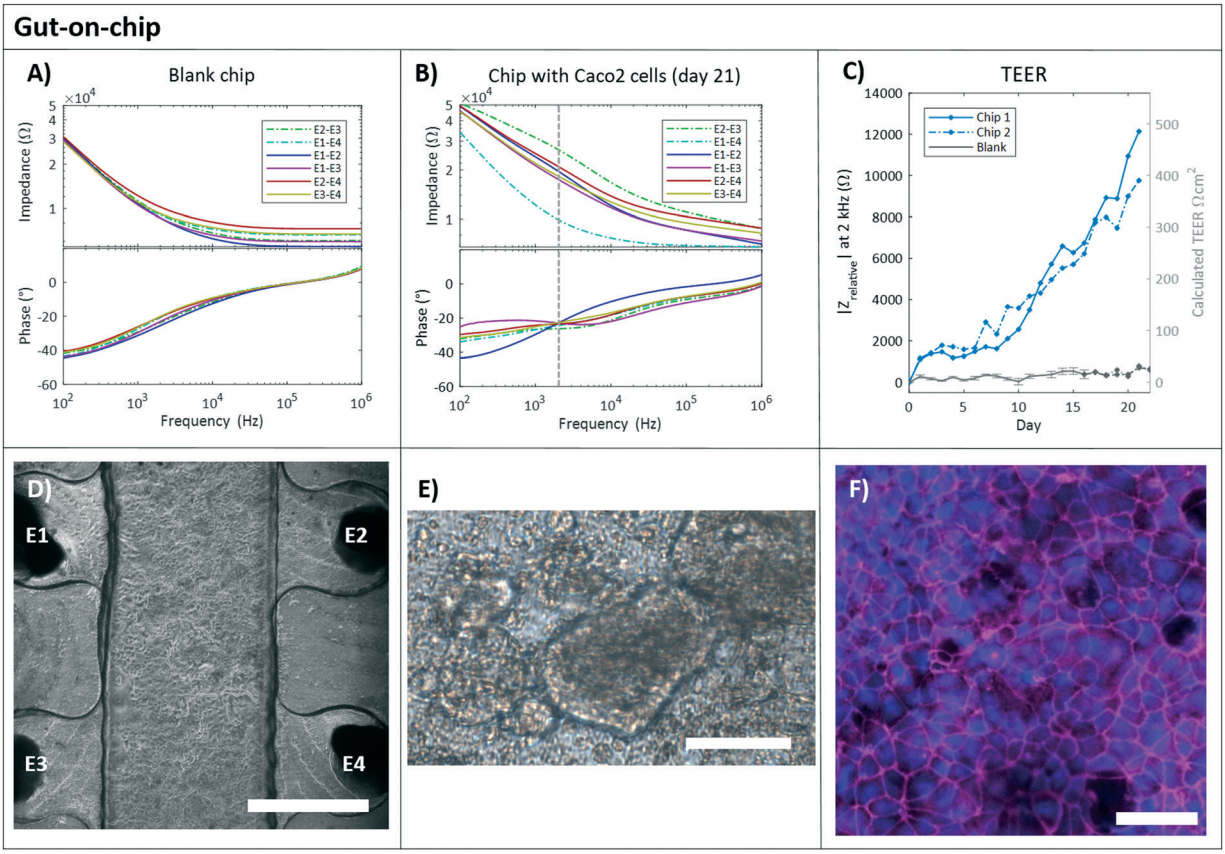

Fig. 3 Gut-on-chip. The typical impedance spectra with magnitude (Ω, top plot) and phase (°, bottom plot) are plotted against the frequency (Hz) for a blank chip containing only DMEM culture medium (A) and a chip with Caco-2 cells cultured for 21 days (B). The continuous lines are the electrode pairs measuring through the PDMS membrane (and cell layer for B), and the dashed lines correspond to the measurements without membrane, between top electrodes (E2–E3) and bottom electrodes (E1–E4). The vertical dashed line indicates the read-out frequency of 2 kHz. C) Relative impedance at 2 kHz of the four electrode pairs measuring through the membrane and cell layer over time in a chip with Caco-2 cells (blue). The day 0 measurement (before cell seeding) was subtracted from all subsequent measurements (n = 2). Also, the relative impedance at 2 kHz of the four electrode pairs measuring through PDMS membrane over time in chips without cells, the blank chips are presented in grey. The day 0 measurement was subtracted from all subsequent measurements. The average of 3 blank chips is shown ± standard deviation (n = 3) up until day 17. At day 17, one chip was excluded from the experiment because after visual inspection leakage at the in- and outlets of the chip was observed. D) Gut-on-chip lined with a monolayer of Caco-2 cells (P30) at day 4 of culture. Phase-contrast image, scale bar represents 750 μm. E) Bright field image of Caco-2 cells on chip at day 21, showing not all cells in focus, indicating the formation of a 3D structure. Scale bar represents 75 μm. F) Immunofluorescence staining indicates the cell nuclei (NucBlue, blue) and tight junction protein ZO-I (magenta) of the Caco-2 cells at day 21. Scale bar represents 50 μm.

an increasing trend such as we observed in Fig. 3C, which could be explained by the difference between cell culture on chips and on Transwell systems. Caco-2 cells are known, as they are cancerous cells, to grow in several cell layers or three-dimensional (3D) structures when cultured in a microfluidic channel. Hereby, the resistances between the measuring electrodes will keep increasing and therefore the barrier resistance (TEER) will keep increasing. The formation of 3D structures was also observed in our gut-on-chips, starting from the 8th day of culture, with a phase-contrast microscope, and shown in Fig. 3E. Our measured TEER values are in accordance with this observation, as we see a steeper increase of measured TEER particularly after 10 days of culture (Fig. 3C). We cannot compare the observed trend with microfluidic culture systems presented, as most microfluidic experiments usually culture only up to 10 or 12 days,[11,19,21,41] while it was shown previously that more than 15 days are required to form a fully differentiated and confluent cell layer in Transwell systems.[43,44]

On day 21, cells were fixed and stained for nuclei and tight junction protein ZO-1 (Fig. 3F). A dense layer of Caco-2 cells was observed, with indications of villi formation (Fig. 3E). The expression of ZO-I protein is abundantly observed (Fig. 3F), specifically at the plasma membrane at the sites of cell–cell contact, as expected.

Intestinal barrier disruption and recovery. To test whether our system can measure changes in the barrier function and to verify that the measured resistance was related to the formation of the tight junctions, the Caco-2 cell monolayer was disrupted by adding 5 mM EGTA for 45 minutes. EGTA is strong calcium (Ca^{2+}) chelator, which will affect both adherens and tight junctions, resulting in a disrupted paracellular

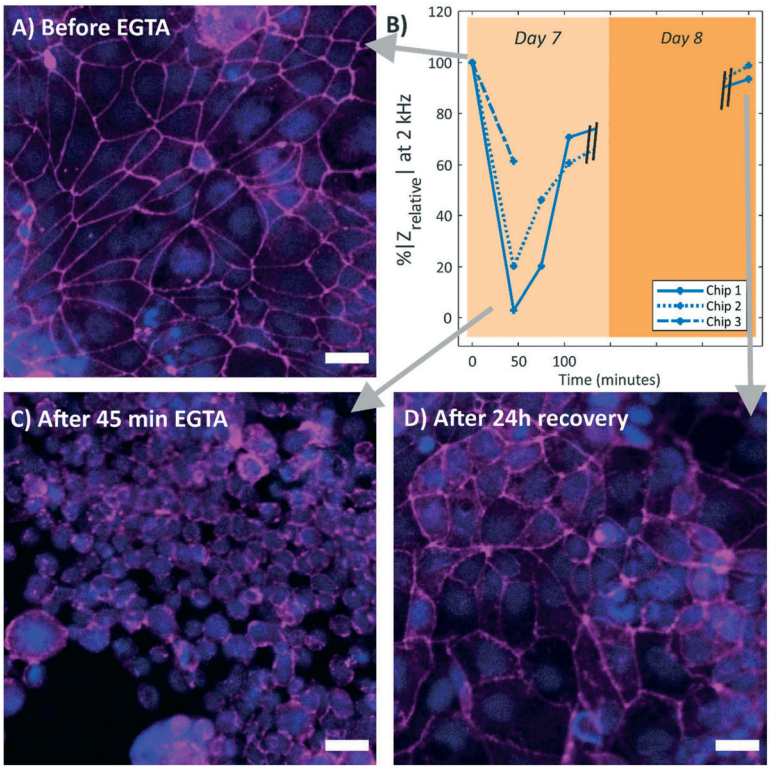

Fig. 4 Response of the Caco-2 barrier function to the treatment of EGTA incubation, in B) the relative impedance at 2 kHz over time in three chips with Caco-2 cells (P31) is shown. All relative impedances were calculated as percentages with respect to the relative impedance at day 7 (n = 3), before EGTA treatment. A decrease in impedance was observed after 45 minutes of EGTA treatment, followed by an increase in impedance during incubation in DMEM. The impedance almost fully recovered overnight. Chip 3 is fixated after EGTA treatment, therefore this chip has only two measurements. Immunofluorescence staining of the cell nuclei (NucBlue, blue) and tight junction protein ZO-1 (magenta) at different time points during the EGTA treatment. A) Caco-2 cells before EGTA treatment, with clear indication of the ZO-1 proteins at the cell–cell borders. C) Caco-2 cells directly after 45 minutes of EGTA treatment, without this clear cell–cell border. The cell monolayer looks disrupted. D) Caco-2 cells after 24 hours recovery in DMEM, the ZO-1 protein is again observed at the cell–cell borders. All scale bars represent 30 μm.

barrier function of the tissue barrier.[17] Fig. 4 shows the effect of the treatment with EGTA. The measured magnitude showed a reduction of ~70% (average of the three chips) with respect to the measurement before adding EGTA, indicating a loss of barrier function (Fig. 4B). Subsequent incubation with DMEM provides calcium ions to recover the cellular junctions and thus the barrier function. The measured impedance reached after overnight recovery to almost 100%, indicating a full recovery of the barrier function (Fig. 4B). This response is similar to a gut-on-chip system with integrated sensors earlier presented by Henry *et al.*[17]

Additionally, to correlate the measured TEER with an immunofluorescence staining of the tight junction proteins, the chips were fixed and stained at three different time points: before EGTA treatment (Fig. 4A), directly after 45 minutes of EGTA treatment (Fig. 4C), and after 24 hour recovery in DMEM (Fig. 4D). Clearly, a correlation between the presence of tight junction protein ZO-1 at the cell periphery and the measured TEER can be seen, demonstrating the effectiveness of our system. This experiment proves that we were specifically measuring the tissue barrier (TEER) in our chip.

The gut-on-chips shown in Fig. 3 were also treated with EGTA at day 19 of culture. The measured TEER also indicates a loss of barrier function and overnight recovery to more than 100%, see ESI† S3.

BBB-on-chip

The same procedure was performed for measuring the barrier function of the hCMEC/D3 cells. For 4 days the impedance was recorded at RT EGM in the chips with and without cells. The readout frequency for the hCMEC/D3 cells was chosen at 20 kHz (Fig. S5†).

The hCMEC/D3 cells in a microfluidic chip are known to develop under static culture conditions a low to medium level of TEER of 5–50 Ω cm^2.[31,45,46] The barrier formation of the hCMEC/D3 cells over 4 days is shown in Fig. 5. The calculated TEER increased up to 30 Ω cm^2, which is in agreement with other studies.[20,21,29,47,48] However, after 4 days of culture, the TEER values did not reach the plateau as reported previously.[20,47] This may be due to the cellular transmigration through the 5 μm pores to another side of the membrane.[49] Additionally, astrocytes are known to influence the tightness of the BBB, therefore the co-culture can be performed in the future to enhance the barrier property and mimic more functional BBB.[50,51]

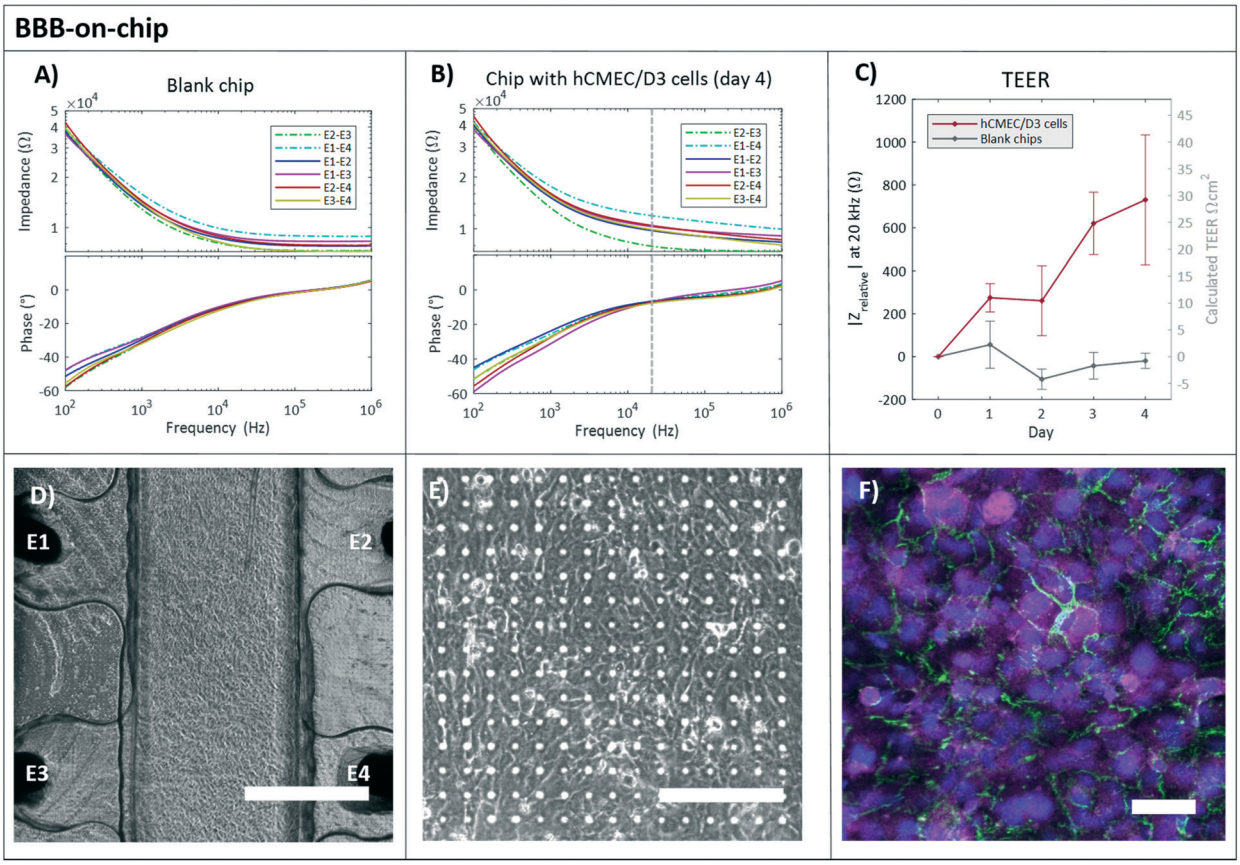

Fig. 5 BBB-on-chip. Typical impedance spectra of the BBB-on-chip. The impedance magnitude (Ω, top plot) and phase (°, bottom plot) are plotted against the frequency (Hz) for a blank chip containing only EGM culture medium (A) and a chip with hCMEC/D3 cells cultured for 4 days (B). The continuous lines are the electrode pairs measuring through the PDMS membrane (and cell layer for B), and the dashed lines correspond to the measurements without membrane, between top electrodes (E2–E3) and bottom electrodes (E1–E4). The vertical dashed line indicates the read-out frequency of 20 kHz. C) Relative impedance at 20 kHz of the four electrode pairs measuring through the membrane and cell layer over time in chips with hCMEC/D3 cells (red). The day 0 measurement (before cell seeding) was subtracted from all subsequent measurements (n = 3). Also, the relative impedance at 20 kHz of measurements in chips without cells, blank chips (grey) are shown (n = 3). The averages of 3 chips with and without cells is shown ± standard deviation. D) A phase-contrast image of the channel lined with hCMEC/D3 cells cultured for 4 days (scale bar represents 750 μm) and a close-up image E) presenting a clear view on the cells cultured on the transparent membrane. Scale bar represents 150 μm. F) Immunofluorescent staining of the cells with ZO-1 (magenta), VE-Cadherin (green) and NucBlue (blue). Scale bar represents 50 μm.

In the chips without cells, the resistance of the system did not change over time and the measured relative impedance remained relatively stable around 0 Ω, which is shown in Fig. 5C (grey line). The presented variation in the empty chips may be due to the change in the physical parameters (*e.g.* temperature, pH, medium composition, and others).

The immunofluorescence indicated the tight barrier development with positive ZO-1 and VE-cadherin expression after 4 days of culture (Fig. 5F).

Conclusions

In this paper, we presented a cleanroom-free, versatile fabrication method for the integration of platinum electrode wires in a PDMS OoC that allowed us to monitor the barrier function in real-time using impedance spectroscopy. The presented fabrication method allows abundant design freedom, and the electrode configuration allows visual inspection at the sites of the electrodes and the possibility to multiplex both the electrodes and the number of OoCs in one PDMS device. We monitored and observed the formation of the cell barrier in a gut-on-chip during a 8 day and 21 day cell culture. The capability and sensitivity of our system were checked by disrupting the epithelial cell-barrier with EGTA treatment. The recorded TEER values indicated a clear loss in barrier tightness and subsequent recovery of the barrier overnight in DMEM. The disruption and recovery event were supported with an immunofluorescence staining, demonstrating the effectiveness of our measuring method and chip. We also monitored the barrier function in a BBB-on-chip, demonstrating that our proposed PDMS two-layer OoC can be used to monitor the barrier function with different cell types forming a monolayer or tissue barrier, providing a valuable tool for studies to barrier targeting drug development.

Author contributions

E. B. developed and fabricated the design of the chip. M. Z. fabricated the thin PDMS membranes. E. B. and M. Z. performed experimental work, data processing and wrote the manuscript. D. B. provided resources and input to the manuscript. M. O. and L. S. supervised and contributed to writing, reviewing, and editing of the manuscript.

Conflicts of interest

Authors declare no conflicts of interest.

Acknowledgements

This work was funded by a Building Blocks of Life grant from the Netherlands Organization for Scientific Research (NWO), grant no. 737.016.003 and by the Netherlands Organ-on-Chip Initiative (NOCI), an NWO Gravitation Project funded by the Ministry of Education, Culture and Science of the Government of the Netherlands, under grant no. 024.003.001.

References

1 S. N. Bhatia and D. E. Ingber, *Nat. Biotechnol.*, 2014, **32**, 760–772.
2 N. Isoherranen, R. Madabushi and S. Huang, *Clin. Transl. Sci.*, 2019, **12**, 113–121.
3 L. A. Low, C. Mummery, B. R. Berridge, C. P. Austin and D. A. Tagle, *Nat. Rev. Drug Discovery*, 2020, 1–17.
4 B. Zhang, A. Korolj, B. F. L. Lai and M. Radisic, *Nat. Rev. Mater.*, 2018, **3**, 257–278.
5 D. E. Ingber, *Cell*, 2016, **164**, 1105–1109.
6 C. M. Sakolish, M. B. Esch, J. J. Hickman, M. L. Shuler and G. J. Mahler, *EBioMedicine*, 2016, **5**, 30–39.
7 Y. B. Arlk, M. W. Van Der Helm, M. Odijk, L. I. Segerink, R. Passier, A. Van Den Berg and A. D. Van Der Meer, *Biomicrofluidics*, 2018, **12**(4), 042218.
8 L. Shuler and J. J. Hickman, *TEER measuments in cells*, 2016, vol. 20.
9 R. Kim, P. J. Attayek, Y. Wang, K. L. Furtado, R. Tamayo, C. E. Sims and N. L. Allbritton, *Biofabrication*, 2019, **12**(1), 015006.
10 K. Benson, S. Cramer and H. J. Galla, *Fluids Barriers CNS*, 2013, **10**, 1–11.
11 H. J. Kim, D. Huh, G. Hamilton and D. E. Ingber, *Lab Chip*, 2012, **12**, 2165–2174.
12 W. Shin, A. Wu, M. W. Massidda, C. Foster, N. Thomas, D. W. Lee, H. Koh, Y. Ju, J. Kim and H. J. Kim, *Front. Bioeng. Biotechnol.*, 2019, **7**, 1–13.
13 M. Odijk, A. D. Van Der Meer, D. Levner, H. J. Kim, M. W. Van Der Helm, L. I. Segerink, J. P. Frimat, G. A. Hamilton, D. E. Ingber and A. Van Den Berg, *Lab Chip*, 2015, **15**, 745–752.
14 J. Yeste, X. Illa, C. Gutiérrez, M. Solé, A. Guimerà and R. Villa, *J. Phys. D: Appl. Phys.*, 2016, **49**(37), 375401.
15 A. Asif, K. H. Kim, F. Jabbar, S. Kim and K. H. Choi, *Microfluid. Nanofluid.*, 2020, **24**, 1–10.
16 R. Booth and H. Kim, *Lab Chip*, 2012, **12**, 1784–1792.
17 O. Y. F. Henry, R. Villenave, M. J. Cronce, W. D. Leineweber, M. A. Benz and D. E. Ingber, *Lab Chip*, 2017, **17**, 2264–2271.
18 B. M. Maoz, A. Herland, O. Y. F. Henry, W. D. Leineweber, M. Yadid, J. Doyle, R. Mannix, V. J. Kujala, E. A. Fitzgerald, K. K. Parker and D. E. Ingber, *Lab Chip*, 2017, **17**, 2294–2302.
19 M. W. van der Helm, O. Y. F. Henry, A. Bein, T. Hamkins-Indik, M. J. Cronce, W. D. Leineweber, M. Odijk, A. D. van der Meer, L. I. Segerink and D. E. Ingber, *Lab Chip*, 2019, **19**, 452–463.
20 M. W. van der Helm, M. Odijk, J.-P. Frimat, A. D. van der Meer, J. C. T. Eijkel, A. van den Berg and L. I. Segerink, *Biosens. Bioelectron.*, 2016, **85**, 924–929.
21 F. R. Walter, S. Valkai, A. Kincses, A. Petneházi, T. Czeller, S. Veszelka, P. Ormos, M. A. Deli and A. Dér, *Sens. Actuators, B*, 2016, **222**, 1209–1219.
22 J. Yeste, L. Martínez-Gimeno, X. Illa, P. Laborda, A. Guimerà, J. P. Sánchez-Marín, R. Villa and I. Giménez, *Biotechnol. Bioeng.*, 2018, **115**, 1604–1613.
23 M. W. van der Helm, M. Odijk, J. P. Frimat, A. D. van der Meer, J. C. T. Eijkel, A. van den Berg and L. I. Segerink, *J. Visualized Exp.*, 2017, **2017**, 1–8.
24 M. Zakharova, M. A. Palma do Carmo, M. W. van der Helm, H. Le-The, M. N. S. de Graaf, V. Orlova, A. van den Berg, A. D. van der Meer, K. Broersen and L. I. Segerink, *Lab Chip*, 2020, **20**, 3132–3143.
25 B. Srinivasan, A. R. Kolli, M. B. Esch, H. E. Abaci, M. L. Shuler and J. J. Hickman, *J. Lab. Autom.*, 2015, **20**, 107–126.
26 R. B. Van Breemen and Y. Li, *Expert Opin. Drug Metab. Toxicol.*, 2005, **1**, 175–185.
27 H. J. Kim and D. E. Ingber, *Integr. Biol.*, 2013, **5**, 1130–1140.
28 D. E. Eigenmann, G. Xue, K. S. Kim, A. V. Moses, M. Hamburger and M. Oufir, *Fluids Barriers CNS*, 2013, **10**(33), 1–17.
29 B. B. Weksler, E. A. Subileau, N. Perrière, P. Charneau, K. Holloway, M. Leveque, H. Tricoire-Leignel, A. Nicotra, S. Bourdoulous, P. Turowski, D. K. Male, F. Roux, J. Greenwood, I. A. Romero and P. O. Couraud, *FASEB J.*, 2005, **19**, 1872–1874.
30 B. P. Daniels, L. Cruz-Orengo, T. J. Pasieka, P. O. Couraud, I. A. Romero, B. Weksler, J. A. Cooper, T. L. Doering and R. S. Klein, *J. Neurosci. Methods*, 2013, **212**, 173–179.
31 B. Weksler, I. A. Romero and P. O. Couraud, *Fluids Barriers CNS*, 2013, **10**, 1–10.
32 D. Huh, H. J. Kim, J. P. Fraser, D. E. Shea, M. Khan, A. Bahinski, G. A. Hamilton and D. E. Ingber, *Nat. Protoc.*, 2013, **8**, 2135–2157.
33 E. Tanumihardja, R. H. Slaats, A. D. Van Der Meer, R. Passier, W. Olthuis and A. Van Den Berg, *ACS Sens.*, 2021, **6**, 267–274.
34 E. Tanumihardja, A. P. Rodríguez, J. T. Loessberg-zahl, B. Mei, W. Olthuis and A. Van Den Berg, *Sens. Actuators, B*, 2021, **334**, 129631.

35 F. van Rossem, J. G. Bomer, H. L. de Boer, Y. Abbas, E. de Weerd, A. van den Berg and S. Le Gac, *Sens. Actuators, B*, 2017, **238**, 1008–1016.
36 S. J. Kim, H. Jung, C. Lee, M. H. Kim and Y. Lee, *Sens. Actuators, B*, 2014, **191**, 298–304.
37 E. E. Krommenhoek, M. van Leeuwen, H. Gardeniers, W. M. van Gulik, A. Van Den Berg, X. Li, M. Ottens, L. A. M. van der Wielen and J. J. Heijnen, *Biotechnol. Bioeng.*, 2008, **99**, 884–892.
38 C. Drieschner, N. T. K. Vo, H. Schug, M. Burkard, N. C. Bols, P. Renaud and K. Schirmer, *Cytotechnology*, 2019, **71**, 835–848.
39 A. Béduneau, C. Tempesta, S. Fimbel, Y. Pellequer, V. Jannin, F. Demarne and A. Lamprecht, *Eur. J. Pharm. Biopharm.*, 2014, **87**, 290–298.
40 C. Huang, Q. Ramadan, J. B. Wacker, H. C. Tekin, C. Ruffert, G. Vergères, P. Silacci and M. A. M. Gijs, *RSC Adv.*, 2014, **4**, 52887–52891.
41 H. Y. Tan, S. Trier, U. L. Rahbek, M. Dufva, J. P. Kutter and T. L. Andresen, *PLoS One*, 2018, **13**, 1–23.
42 J. Wegener, S. Zink, P. Rösen and H. J. Galla, *Pflugers Arch. PFLUG Arch. Eur. J. Phy.*, 1999, **437**, 925–934.
43 L. Fredlund, S. Winiwarter and C. Hilgendorf, *Mol. Pharmaceutics*, 2017, **14**, 1601–1609.
44 I. Hubatsch, E. G. E. Ragnarsson and P. Artursson, *Nat. Protoc.*, 2007, **2**, 2111–2119.
45 K. Hatherell, P. O. Couraud, I. A. Romero, B. Weksler and G. J. Pilkington, *J. Neurosci. Methods*, 2011, **199**, 223–229.
46 S. Hinkel, K. Mattern, A. Dietzel, S. Reichl and C. C. Müller-Goymann, *Int. J. Pharm.*, 2019, **566**, 434–444.
47 L. M. Griep, F. Wolbers, B. De Wagenaar, P. M. Ter Braak, B. B. Weksler, I. A. Romero, P. O. Couraud, I. Vermes, A. D. Van Der Meer and A. Van Den Berg, *Biomed. Microdevices*, 2013, **15**, 145–150.
48 E. Urich, S. E. Lazic, J. Molnos, I. Wells and P. O. Freskgård, *PLoS One*, 2012, **7**(5), e38149.
49 E. Vandenhaute, A. Drolez, E. Sevin, F. Gosselet, C. Mysiorek and M. P. Dehouck, *Lab. Invest.*, 2016, **96**, 588–598.
50 K. Sobue, N. Yamamoto, K. Yoneda, M. E. Hodgson, K. Yamashiro, N. Tsuruoka, T. Tsuda, H. Katsuya, Y. Miura, K. Asai and T. Kato, *Neurosci. Res.*, 1999, **35**, 155–164.
51 N. J. Abbott, L. Rönnbäck and E. Hansson, *Nat. Rev. Neurosci.*, 2006, **7**, 41–53.